ATLANTIS PRESS

Advances in Engineering Research, volume 188

International Conference on Aviamechanical Engineering and Transport (AviaENT 2019)

Fractal Model of Elastoplastic Contact of Nominally Flat Rough Surfaces

Tikhomirov V.P.
Department of «Pipeline Transportation Systems»
FSBEI of HE «Bryansk state technical university»
Bryansk, Russia
dm-bgtu@yandex.ru

Izmerov M.A.
Department of «Pipeline Transportation Systems»
FSBEI of HE «Bryansk state technical university»
Bryansk, Russia
m.izmerov@yandex.ru

Abstract- ***The problem of parameter estimation of rough surface contact interaction due to 3D modelling of fractal model contact interaction, when they are satisfactory to initial surfaces, is solved. This approach takes into account surface contour basic parameters that are essentially relevant to the results and accuracy of the calculation.***

Keywords- modeling, contact stiffness, contact interaction, fractal surface, surface contingence, contact patches.

I. INTRODUCTION

Machine part surfaces have a number of properties that characterize their quality. These include topography (macro-declines, surface undulation and surface contour), physical, mechanical and chemical features of the surface coating and afterstrains in the near-surface zones. The contact between two rough surfaces consists of a microcontact set reacting the load and specifying the actual contact area of physical bodies mating. Actual contact area is usually significantly less than the nominal (geometric) contact area, and it is the actual area that determines these important mating parameters: contact stiffness, electrical and thermal conductivity, etc. Therefore, from the point of view of abut operating condition ensuring, it is especially important to specify the contact interaction parameters.

To describe the quality of behavior of surface contour contact in some cases statistical models, the parameters of which depend on the scale [1, 2] are used. The model of surface contour with the parameters being invariant to the scale is presented in works [3, 4]. These works are based on fractal properties; the surface contour (profile) model is described by the Weierstrass – Mandelbrot equation. Majumdar – Bhushan (M-B) model considering the elastoplastic contact, suggests that in the process of contact load increase there should be a plastic contact, which with a further growth in the load, changes into an elastic state and it contradicts the classical approach of Hertz theory.

The authors of the M-B model believe that small inequalities covering the protrusion are deformed plastically and in the process of coalesce with each other form a larger contact patch being in an elastic state. If the protrusion in the M-B model is thought of as a smooth spherical segment in its upper part then the use of Hertz theory for a specific protrusion and transition condition from the elastic state to the elastoplastic is appropriate.

II. MODELS OF FRACTAL SURFACES

To describe fractal models of surface contour we use 3-D Weierstrass - Mandelbrot function:

$$(x,y) = L\left(\frac{G}{L}\right)^{(D_S-2)}\left(\frac{ln\gamma}{M}\right)^{1/2}\sum_{m=1}^{M}\sum_{n=n_1}^{n_{max}}\gamma^{(3-D_S)n}\{\cos\emptyset_{m,n} -$$

$$-cos\left[\frac{2\pi\gamma^n(x^2+y^2)^{1/2}}{L}\right]\cos\left(arctg\left(\frac{y}{x}\right)-\frac{\pi m}{M}\right)+\emptyset_{m,n}\Big\}$$

Here $2<D_S<3$ is the fractal dimension of the surface; G is the fractal roughness; γ =1.5; $L=1/\gamma^{n1}$ is the length of the profile under consideration; $\emptyset_{m,n}$ is a random variable distributed equally on the interval $[0, 2\pi]$; n_{max}= int $[\lg(L/L_S) / \lg\gamma]$ is the integral of the upper limit of the sum; L_S is the length fitting the size of the gage rod.

Fig. 1 shows models of fractal surfaces: a) – with fractal dimension D = 2.2, b) – D = 2.5, c) – D = 2.8. Model of a protrusion (Fig. 2) is presented in the form of a cosine curve. When interacting with a smooth die block, the upper part in the form of a spherical segment is deformed, while the area of the real contact has a radius r < r'.

We assume that for an isotropic surface it is the profile described by the following expression (for y=0) that is informative:

$$z(x=0) = G^{(D_S-2)}(ln\gamma)^{1/2}l^{(3-D_S)}\left[\cos\emptyset_{m,n} - cos\left(\frac{2\pi x}{l}-\emptyset_{m,n}\right)\right].$$

The height of the protrusion, represented as a fractal object, is equal to:

$$\delta = G^{(D_S-2)}(ln\gamma)^{1/2}l^{(3-D_S)}.$$

The radius of the protrusion upper part curvature is determined by the formula (Majumdar – Bhushan model):

$$R' = \frac{1}{\left|\frac{d^2z(x=0)}{dx^2}\right|} = \frac{l^{(D_S-1)}}{4\pi^2G^{(D_S-2)}(ln\gamma)^{\frac{1}{2}}}. \qquad (1)$$

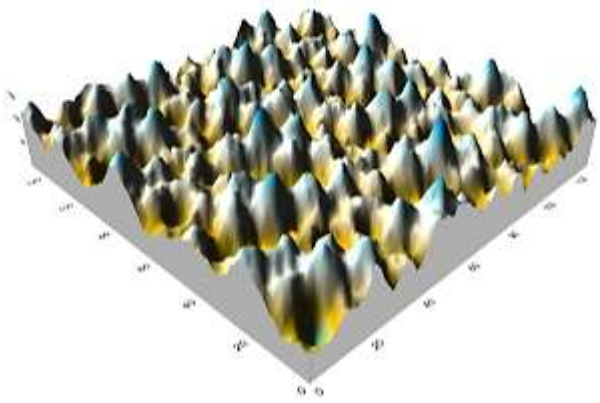

a)

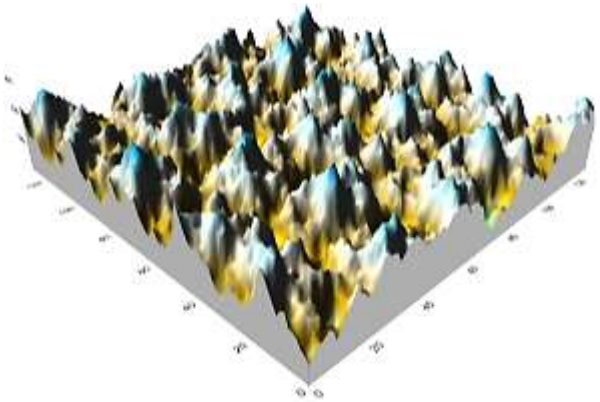

b)

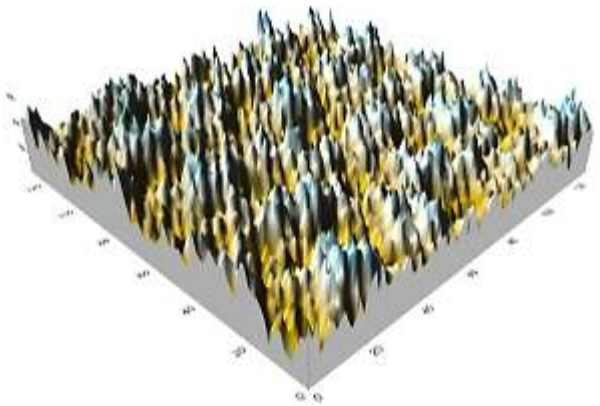

c)

Fig. 1. Models of fractal surfaces with different fractal dimensions: a) D = 2.2, b) D = 2.5, c) D = 2.8

In this case, the rough surface model is represented as a set of spherical segments located on the middle plane and having statistically distributed heights. Provided that the radii of the protrusion upper parts are of equivalent grade the rough surface is described within the Greenwood-Williamson model. In actuality the problems of friction and wear take into consideration the protrusion upper part deformation, for which the radius of curvature will be different in contrast to the model M-B (Fig. 2).

Imagine a protrusion in the form of a cone and we'll have:

$$\frac{4\pi r'^2}{\pi l^2} = \frac{\omega}{\delta}. \quad (2)$$

After deformation of the upper part of the protrusion, the actual contact area $\boldsymbol{a}$ at the elastic state of the contact is equal to:

$$\pi r'^2 = 2a. \quad (3)$$

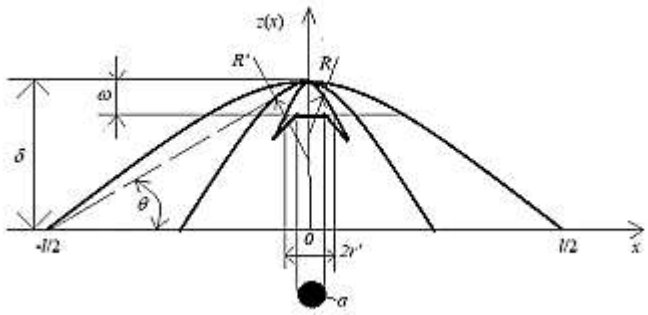

Fig. 2. Model of protrusion

Inserting the expression (3) into equation (2), we will have:

$$\frac{8a}{\pi l^2} = \frac{\omega}{\delta}.$$

At the same time $\omega \cong r' tg\Theta$; $\delta = (l/2)tg\Theta$. Further:

$$\frac{\omega}{\delta} = \frac{2r'}{l} = \frac{8a}{l^2}$$

or:

$$\frac{4a}{\pi l} = r'. \quad (4)$$

We'll change the equation (4) as follows:

$$\left(\frac{4a}{\pi l}\right)^2 = r'^2 \cdot \frac{\pi}{\pi}.$$

From which:

$$l = \left(\frac{8a}{\pi}\right)^{1/2}. \quad (5)$$

Inserting the expression (5) into equation (1), we'll have:

$$R = \frac{(8a)^{(D_S-1)/2}}{4\pi^{(3+D_S)/2} G^{(D_S-2)} (ln\gamma)^{\frac{1}{2}}}. \quad (6)$$

III. THE MODEL OF CONTACT INTERACTION

Unlike the M-B model, the protrusion shown in Fig. 2 and having a certain radius of curvature in the upper part, it is

deformed first elastically, and then with an increase in the load it is distorted plastically. The Majumdar – Bhushan (M-B) model assumes that contact patches, having an area that is greater than some critical value of $a > a_c$, are in an elastic state from the beginning of deformation $\delta < \delta_c$. Contact patches with an area of $a < a_c$ are plastically distorted by deformation $\delta > \delta_c$. In the process of spreading, they approach each other and it results in both: a growth of contact patches and a transition from plastic to elastic contact. Majumdar and Bhushan believe that "due to the fact that smaller contact patches have smaller curve radius, so they will more likely undergo plastic deformation". This result contradicts classical contact mechanics, that is either Hertz theory or the Greenwood – Williamson model (G-W). The reason for this discrepancy lies in the assumption, that patch area $a \equiv l^2$ and $\omega \equiv \delta$ in the model M-B [5]. Protrusion model (Fig. 2) implies the presence of a smooth spherical segment at the top in deformation of unevenness being $0 \le \omega \le \delta$. Radius of the upper part of the protrusion R differs from either M-B or G-W models. We believe that, unlike M-B model, the elastic contact fulfils the condition $\omega < \omega_c$ and $a < a_c$, while the plastic contact obeys the condition of $\omega > \omega_c$ and $a > a_c$ and that is in agreement with classical mechanical principles of contact interaction. With an increase in the load on the flat die we have the following stages of the protrusion deformation: elastic, elastoplastic - 1, elastic-plastic - 2 and plastic. We believe that in order to simplify the problem there are only two types of the state: elastic and plastic.

The relation between the load and the contact patch area is as follows:

- for elastic contact

$$F^0{}_e = \frac{4}{3} E R^{\frac{1}{2}} \omega^{\frac{3}{2}} = \frac{4}{3} E R^{\frac{1}{2}} \left(\frac{a}{\pi R}\right)^{\frac{3}{2}} = \frac{4 E a^{\frac{3}{2}}}{3 \pi^{\frac{3}{2}} R}; \quad \frac{1}{E} = \frac{1-\mu_1^2}{E_1} + \frac{1-\mu_2^2}{E_2};$$

- for plastic contact

$$F_p = Ha; \quad H = min\{H_1, H_2\}.$$

Here: E_1, E_2, μ_1, μ_2 are elastic moduli, Poisson's ratios of physical agents' tying-in; H – hardness.

Inserting the radius expressed by the equation (6) into the ratio for the elastic contact, we have:

$$F^0{}_e = \frac{2^{(11-3D_S)/2}}{3} E \pi^{(D_S/2)} G^{(D_S-2)} (ln\gamma)^{1/2} a^{(4-D_S)/2} = Q\, a^{(4-D_S)/2}.$$

Here:

$$Q = \frac{2^{(11-3D_S)/2}}{3} E \pi^{(D_S/2)} G^{(D_S-2)} (ln\gamma)^{1/2}.$$

The transition criterion is determined on the basis of equality $F_e = F_p$. Setting equal load of both elastic and plastic states, we will have the following expression after the transformation of the critical value of the contact patch area:

$$a_c = \left[\frac{9}{256\pi}\left(\frac{H}{E}\right)^2 \frac{8^{(D_S-1)}}{G^{2(D_S-2)} ln(\gamma)}\right]^{1/(2-D_S)}.$$

Multiple contact. Figure 3 shows milling and abrasive surface matching (top) and two abrasive surfaces (bottom), as well as contact areas mating them. The actual contact area is the product of the number of actual spots and the average contact patch area:

$$A_r = N(a > a_{min})\langle a \rangle.$$

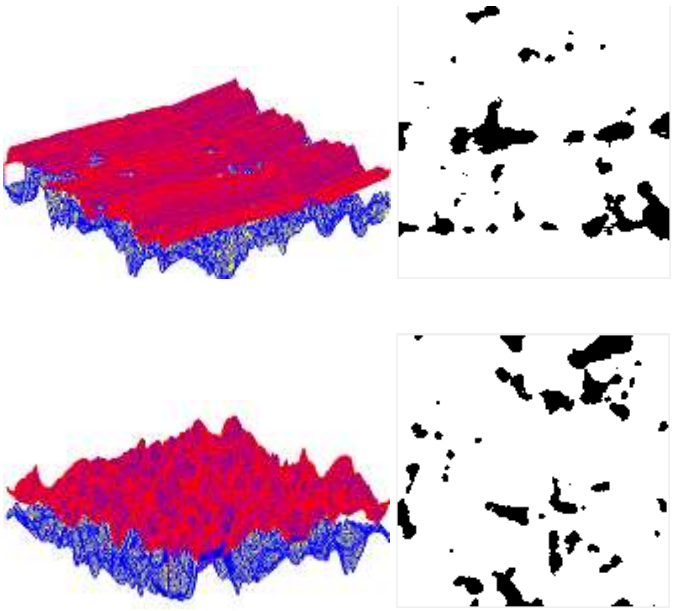

Fig. 3. Rough surfaces matching and their contact patches: milling and abrasive (above), and two abrasive (below)

The number of spots being greater than the minimum value is estimated by [3]

$$N(a > a_{min}) = \left(\frac{a_{max}}{a_{min}}\right)^{(D_S-1)/2} = \left(\frac{a_{max}}{a_{min}}\right)^{D/2}, \quad D = D_S - 1.$$

We shall find the average area of the contact patches, denoting a dimensionless area expressed in terms of $a^* = \frac{a}{a_{max}}$:

$$\langle a \rangle = a_{max} \int_0^1 a^{*\prime} f(a^{*\prime}) da^{*\prime}. \qquad (7)$$

Taking the differential distribution function of the relative contact areas [6] as:

$$f(a^*) = (1-\alpha) a^{*(-\alpha)}$$

inserting it in equation (7), we shall write:

$$\langle a \rangle = a_{max} \frac{1-\alpha}{2-\alpha}.$$

The exponent α is defined as follows. We simulate mating fractal surfaces (Fig. 1) and the get contact patch. We find the areas of contact patches and construct an empirical distribution function, the approximation of which is written as:

$$F(a^*) = a^{*(1-\alpha)}.$$

Finally, we shall write the expression for the actual contact area:

$$A_r = \frac{a_{max}^{(1+D/2)}}{a_{min}^{D/2}} \frac{1-\alpha}{2-\alpha}.$$

The elastic and plastic parts of the actual contact area are measured by the following functional connections:

$$A_{re} = \frac{a_{max}^{\left(1+\frac{D}{2}\right)}}{a_{min}^{\frac{D}{2}}} \frac{1-\alpha}{2-\alpha} \left(a_c^*\right)^{(2-\alpha)},$$

$$A_{rp} = \frac{a_{max}^{(1+D/2)}}{a_{min}^{D/2}} \frac{1-\alpha}{2-\alpha} \left[1 - \left(a_c^*\right)^{(2-\alpha)}\right].$$

Now: $a_c^* = a_c / a_{max}$.

IV. THE RESULT OF COMPUTER SIMULATION OF CONTACT INTERACTION OF SURFACES

The elastic contact is determined by the expression:

$$F_e = \left(\frac{a_{max}}{a_{min}}\right)^{\frac{D}{2}} \int_0^{a^*} Q a^{*\prime \frac{(3-D)}{2}} a_{max}^{\frac{(3-D)}{2}} (1-\alpha) a^{*\prime(-\alpha)} da^{*\prime}$$

$$= \frac{a_{max}^{\frac{3}{2}}}{a_{min}^{\frac{D}{2}}} Q \frac{2(1-\alpha)}{(5-D-2\alpha)} a^{*\frac{(5-D-2\alpha)}{2}}; \quad (8)$$

$$0 \le a^* \le a_c^* = 1.$$

Functional connection $F_e(a^*)$ presented in fig. 4 is deduced in the following way: R_a = 1,2 mym; $G = 6 \cdot 10^{-6}$ mm; $D = 1{,}5$; $D_S = 2{,}5$; $\alpha = 0{,}5$; Q = 731,42 mm$^{1/2}$; $E = 10^5$ MPa; H = 2000 MPa; $a_{max} = a_c$ =5,769 $\cdot 10^{-4}$mm^2; $a_{min} = 10^{-3}$ a_{max}; $a^* = a/a_c$.

Plastic contact takes place at $a \ge a_c$. The expression for the patches in the plastic state we present in the form:

$$F_p = \left(\frac{a_{max}}{a_{min}}\right)^{\frac{D}{2}} H \int_{a_c^*}^{a^*} a^{*\prime} a_{max} (1-\alpha) a^{*\prime(-\alpha)} da^{*\prime} =$$

$$= \frac{a_{max}^{\left(1+\frac{D}{2}\right)}}{a_{min}^{\frac{D}{2}}} H \frac{1-\alpha}{2-\alpha} \left[a^{*(2-\alpha)} - a_c^{*(2-\alpha)}\right], \qquad a_c^* \le a^* \le 1.$$

Besides using previously taken initial data we shall assume a_{max} = [50;75;100] a_c, we shall find: a_{maxi}= 50·5,769·10^{-4}; 75·5,769·10^{-4}; 100·5,769·10^{-4}.

The dimensionless critical area of the patch will be equal to:

$$a_{ci}^* = 1/50; 1/75 \text{ и } 1/100.$$

Evaluation of the nominal area. The dependence of the relative area (bearing area) *Ar/Aa* on the contingence is determined by the expression:

$$\frac{A_r}{A_a} = 0{,}5 erfc\left(\frac{Y}{\sqrt{2}R_q}\right),$$

where: A_r - the actual contact area; A_a - nominal (geometric) area; $erfc(\dots)$ - error function; Y - the distance between the mean plane of datum rough surface and a flat die; R_q – average quadratic deviation of outline ordinates.

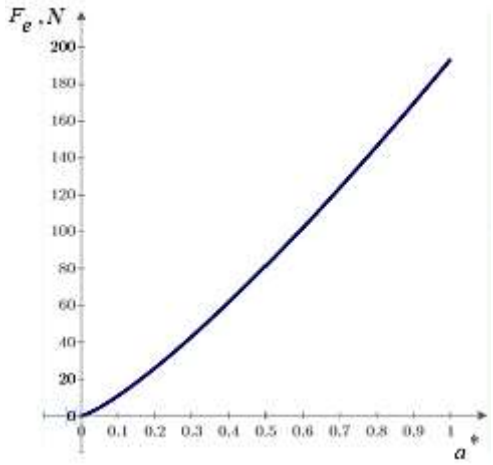

Fig. 4. Load behavior assimilated by elastically deformed contact patches depending on the dimensionless area

As the distance Y is reduced (while convergence increases), the bearing area grows. At Y = 0 the function $erfc(0) = 1$ и $A_a = 2A_r$. the Actual area, consisting of individual patches is determined by the expression quoted above:

$$A_r = \frac{a_{max}^{(1+D/2)}}{a_{min}^{D/2}} \left(\frac{1-\alpha}{2-\alpha}\right), \qquad 1 < D < 2.$$

The maximum area of the contact patch in accordance with Fig. 2 when z(x) = 0 is equal to:

$$a_{max} = \pi \left(R_p tg\theta\right)^2.$$

Here: R_p is the smoothing height; $tg\theta = \Delta q$ *is* the slope of the unevenness with towards the midline.

At the same time:

$$a_{max} = \pi \left(\frac{S_m}{4}\right)^2,$$

where S_m - is statistical estimate of roughness width along the midline.

Fig. 5 shows special intersection points (zeros) of the section-gage log with the midline. The roughness width along the midline is defined directly by the number of zeros *n* (0) designated as the selected length of the profile line:

$$S_m = \frac{2}{n(0)}.$$

The average values of number of zeros (mm^{-1}) fitting in any given processing type (tbl. 1) are provided below [7].

Fig. 5. Special points of section-gage log

TABLE I. THE AVERAGE VALUES OF THE NUMBER OF ZEROS AND THE AVERAGE PITCH

Type of processing	R_q, μm	R_a, μm	R_{max}, μm	$n(0)$, mm^{-1}	S_m, μm
Flat grinding	3,25	2,51	11,19	15	133,32
	1,70	1,37	4,25	27	74,08
	1,19	0,89	2,42	34	58,82
	0,73	0,56	1,66	51	39,22
Circular grinding	0,29	0,23	0,79	140	14,28
	0,14	0,11	0,34	163	12,26
Reseat (fitting)	0,13	0,11	0,38	183	10,92

Functional connections (according to J. A. Rudzit) for the average pitch have the form:

$$S_m = \begin{cases} \dfrac{2}{200 - 278R_a}, & R_a \le 0{,}63\ \text{,μm}; \\ \dfrac{2}{43 - 11R_a}, & R_a > 0{,}63\ \text{μm}\ . \end{cases}$$

Taking up $a_{min} = 10^{-3}a_{max};\ \alpha = 0{,}5; D = 1{,}5$ we obtain the following ratio making possible to tie together both: relative area and type of processing (tbl. 2):

$$\frac{A_r}{A_a} = 10^{3D/2}\frac{a_{max}}{3}.$$

TABLE II. THE NOMINAL CONTACT AREA FOR THE FRACTAL MODEL

Type of processing	R_a, μm	S_m, μm	a_{max}, mm^2	A_a, mm^2
Flat grinding	2,51	133,32	$3{,}49\cdot10^{-3}$	0,414
	1,37	74,08	$1{,}07\cdot10^{-3}$	0,126
	0,89	58,82	$6{,}79\cdot10^{-4}$	0,080
	0,56	39,22	$3{,}13\cdot10^{-4}$	0,040

Fig. 6 presents a dependency graph showing how relative area depends on maximum contact patch area (for the surface with $R_a = 1.37$ μm $\alpha = 0{,}5$)

Normal contact stiffness. Analyze the elastic contact. The load taken up by the rough surface is determined through the previously obtained dependence (8):

$$F_e = \frac{a_{max}^{3/2}}{a_{min}^{D/2}} Q \frac{2(1-\alpha)}{(5-D-2\alpha)} a^{*(5-D-2\alpha)/2},\ \ 0 \le a^* \le a_c^* = 1,$$

where $a^* = a/a_{max}$.

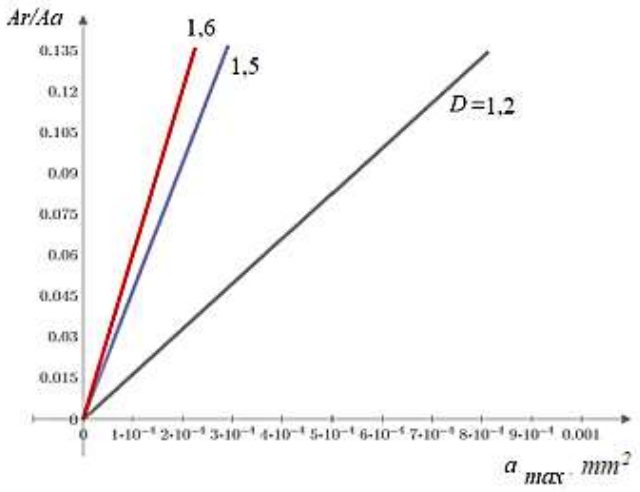

Fig. 6. The dependence of the relative area on the maximum area of the contact patch under different fractal dimension conditions

Making the census of this expression as:

$$F_e = \frac{a_{max}^{\left(\frac{D}{2}+\alpha-1\right)}}{a_{min}^{D/2}} Q \frac{2(1-\alpha)}{(5-D-2\alpha)} a^{(5-D-2\alpha)/2}. \quad (9)$$

Taking the contact stiffness equal to:

$$K_N = \frac{dF_e}{d\omega}.$$

Factoring the relationship between the area of the contact patch a and deformation ω that is written as:

$$a = \pi R\omega.$$

Inserting the value of the radius of the fractal protrusion and modifying the deduced expression with respect to the area of the contact patch, we obtain:

$$a = \frac{2^{3D_S-7}}{[\pi^{D_S+1}G^{2(D_S-2)}(ln\gamma)]^{1/(3-D_S)}}\omega^{2/(3-D_S)}. \quad (10)$$

where D_S = 2,5 we have:

$$a = \frac{\sqrt{2}}{[\pi^{3,5}G(ln\gamma)]^2}\omega^4.$$

Inserting the expression (10) into the equation (9) and making the following development of it taking into account that D_S=D+1, we obtain:

$$F_e = \frac{a_c^{(D+2\alpha-2)/2}}{a_{min}^{D/2}} Q \frac{2(1-\alpha)}{(5-D-2\alpha)} \cdot$$

$$\cdot \left\{\frac{2^{3D_S-7}\omega^{2/(3-D_S)}}{[\pi^{3,5}G^{2(D_S-2)}(ln\gamma)]^{1/(3-D_S)}}\right\}^{(5-D-2\alpha)/2}$$

where D = 1,5 (D_S = 2,5) we get

$$F_e = \frac{a_c^{0,25}}{a_{min}^{0,75}} Q \cdot 0{,}4 \left\{ \frac{\sqrt{2}\,\omega^4}{[\pi^{D_S+1} G (ln\gamma)^2]^2} \right\}^{1,25}.$$

We obtain best possible:

$$F_e = Q^* \omega^5. \quad (11)$$

At this time:

$$Q^* = 2{,}632 \cdot 10^{-4} \frac{a_c^{0,25}}{a_{min}^{0,75}} \frac{Q}{G^{2,5}}.$$

The normal contact stiffness is:

$$K_N = 5 Q^* \omega^4.$$

As an illustration and putting the results obtained earlier by other researchers into perspective we give a numerical example. Let us take the following initial data: R_a = 2.95 μm; α = 0.5; D = 1.5. For grinding finish we estimate the fractal roughness parameter approximately:

$$G = 10^{-5{,}26/R_a^{0,042}} = 10^{-\frac{5{,}26}{2{,}65^{0,042}}} = 9{,}411 \cdot 10^{-6}\, mm.$$

Let's define other parameters:

- the maximum area of elastic contact (according to the formula 10 when hardness of H = 2000 MPa and E = 10^5 MPa) - $a_c = 1{,}419 \cdot 10^{-3}\, mm^2$;
- Q = 916,037 $(\mathrm{H}/mm) mm^{0,5}$;
- $Q^* = 4{,}219 \cdot 10^{15} \left(\frac{\mathrm{H}}{mm^5}\right)$.

Then the contact stiffness is determined by the dependence:

$$K_N = 21{,}095 \cdot 10^{15} \omega^4.$$

Fig. 7 presents a dependency graph showing how contact stiffness depends upon approaching.

Using the expression (11), we find the following dependence of the load upon the approaching for the elastic contact when the following initial data:

D_S =1,585; G = 10^{-9} mm; $a_c = 6{,}956 \cdot 10^{-12}\, mm^2$.

$$F_e = 5{,}59 \cdot 10^{19} \omega^{5{,}819}.$$

The relationship between approaching and load is:

$$\omega = 0.4045 F_e^{0,172}.$$

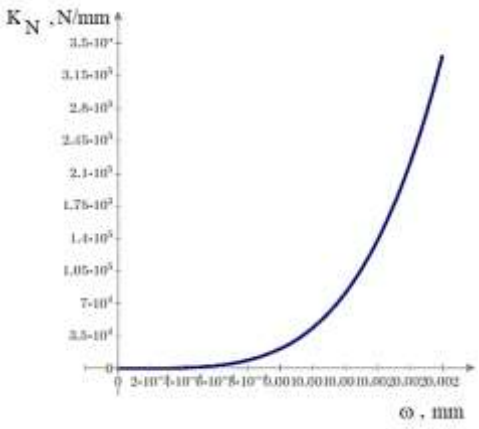

Fig. 7. Dependence of contact stiffness on approaching

Fig. 8 presents the dependences of the approaching upon the load. Comparison of these dependencies is made considering sufficiently similar values of the topographic parameters of the flat joint steel face.

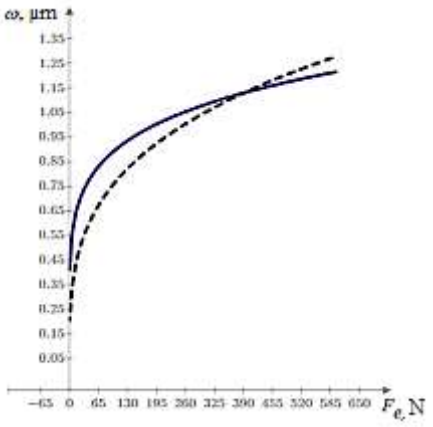

Fig. 8. The dependence of the approaching on the load: full line graph is the fractal model; dashed line is readings of the work [7]

V. CONCLUSION

Thus, the proposed fractal model of contact interaction of the flat joint takes into account those parameters of rough surfaces, which have a significant importance for the result and accuracy of the calculation. These parameters include fractal dimension D and fractal roughness G, which are associated with the roughness parameters according to GOST 2789-73.

References

[1] H. Yang, "Modeling and Analysis of Normal Contact Stiffness of Machined Joint Surfaces," International Journal of Control and Automation, 2014, vol.7, No.6, pp. 21-32.

[2] M. Ciavarella, V. Delfine, G. A. Demelio, "Re-vitalized Greenwood and Williamson model of elastic contact between fractal surfaces", Journal of the Mechanics and Physics of Solids, 2006, Vol. 54(12), pp. 2569–2591.

[3] D. Pavelescu, A. Tudor, “On the roughness fractal character, the tribological parameters and the error factors”, [Proc. of the Romanian Academy. Ser. A.], 2004, Vol. 5, №2.

[4] B. M. Yu, P. Cheng, “A fractal permeability model for bi-dispersed porous media”, In. Journal of Heat and Mass Transfer, 2002, vol. 45, pp. 2983 - 2993.

[5] Cuicui Ji, Wei Jiang,” Revising Elastic-Plastic Contact Models of Fractal Surfaces”, [Proc 5th int. conf. “Measurement, Instrumentation and Automation”]. ICMIA, 2016, pp. 123-129.

[6] V.P. Tikhomirov, M.A. Izmerov, “Distribution of contact patch sizes on rough surfaces”, 2015 [Proc.int. conf. “Mechanical Engineering, Automation and Control Systems”], MEACS, 2015, pp. 1-4.

[7] V.V. Izmailov, D.A. Levyikin, “Normal and shear stiffness of a flat joint of rough surfaces “, Mechanics and physics of the processes on the surface and in contact of solids, parts of processing and power engineering equipment, issue. 5, Tver: TvSTU, 2012, pp. 4 -11.